N

Natural Volatiles & Essential Oils <research.nveo@gmail.com>

mar. 12 sept. 2023 10:26

À moi

Traduire en français

Dear Sir,
Greetings!

Kindly find the attached galley proof of your article entitled **"The interest of a detailed study of thermal signals for thermal safety assessment"**. If you want any changes or corrections please mention them in the same.

Thank you

Regards,
Editorial Assistant
Natural Volatiles & Essential Oils (NVEO) ISSN: 2148-9637
WhatsApp No.: +91 8799769486

Nat. Volatiles & Essent. Oils, 2023;10(1):99-107

NVEO
Natural Volatiles & Essential Oils

The Interest Of A Detailed Study Of Thermal Signals For Thermal Safety Assessment

Hadi Debih[1*], Serge Walter[2]

[1*]Université Mohamed Boudiaf, Laboratoire de Valorisation des Matériaux et Mécanique des Structures, M'sila 28000, Algérie.
[2]Université de Haute Alsace, ENSCMu, LPI-GSEC, 3 Rue A. Werner, F-68093 Mulhouse, France.

***Corresponding Author**: Hadi Debih
Université Mohamed Boudiaf, Laboratoire de Valorisation des Matériaux et Mécanique des Structures, M'sila 28000, Algérie, elhadi.debih@univ-msila.dz

Abstract

Thermal safety assessment of chemicals and chemical processes is based on the interpretation of signals as they would be obtained from a wide set of commercially available devices. Despite the large number of existing techniques devoted to thermal measurements, none of them perfectly fulfils its purpose in view. This is frequently a consequence of the important time constants ruling the heat transfer processes. For any reliable safety assessment, hazardous systems require accurate, both thermodynamic (equilibrium state) and kinetic (transfer rate of energy and matter) characterization. The heat transfer's time is constant; it gives rise to raw thermo-analytical and calorimetric results that nearly always integrate a more or less important contribution of both of these two aspects. The aim of this contribution is to point out some ways to overcome time-constant induced signal modifications and to restore the original information from raw measurements as provided by the available instrument. For safety purposes, it is important to be fully aware of all contributions acting on the signal generation and clearly to distinguish the thermodynamic factors, which are sample size independent from the kinetic factors and which strongly depend on the sample size. Further, the importance of the effect of non-thermal potentials on the thermal behaviour needs to be assessed with regard to unexpected possible dangerous transformations. On hand of a few examples, some main aspects are illustrated with respect to possible erroneous signal interpretation, which could lead to dramatic consequences in thermal process safety assessment applications.

Keywords: Thermal analysis, Calorimetry, Thermal safety, Signal shape, Time constant.

1. Introduction

A thermal measurement is a measurement that concerns heat as the cause or the consequence of transformations of matter. That means, it requires either the determination of the heat *content* of the matter undergoing a transformation or the measurement of the heat *flow* from the sample matter towards its environment. Before trying to carry out any thermal measurement, we must first realize that the only directly measurable thermal magnitude is temperature, which is a potential that is a ratio of energy to an amount of the matter. All other thermal magnitudes, including heat quantity, heat flow, heat capacity, etc. are indirectly derived and basically based on pure temperature measurements. Further, the temperature itself must be converted into another magnitude before becoming usable **[1].** Temperature sensors are based on mechanical deformation (dilatation, phase transition…), on optical or spectroscopic signals (wavelength, radiation intensity, radiant heating) and most often on electrical magnitudes (electrical potential, intensity or resistance) that are the way to render thermal magnitudes compatible with practical measurements for information generation, regulation, recording and control or for safety purposes. The existence of a non-equilibrium steady state necessarily requires a heat flow generating a temperature gradient. In addition, since the thermal sensor, as well as the sample itself can exhibit extremely diverse thermal conductivities and heat transfer properties, the temperature gradients arising from the necessary heat transfer processes can result an important thermal heterogeneity. However, it is not always recommended to enhance the signal power in order to reduce the signal drift or the signal-to-noise ratio, because doing so would modify the content of the signal itself as a

consequence of too important change of working conditions. Besides, the thermal signals always result from more or less dynamic exchange processes. Thus, the measured signals are always delayed by the time constants of both the ongoing physico-chemical processes in the sample and the transfer properties of the sample being measured, the heat transfer interface and the thermal sensors. Such contribution will give some insight into the origins and the practical consequences of these aspects **[2].**

2. Fundamentals. The importance of time constants for thermal measurements.

Since any temperature sensor just gives a measurement of its own temperature, it is essential to know the relationship linking the sensor temperature to the actual source temperature. Therefore, one must keep in mind that the sensor temperature requires a heat flow for changing its own temperature. This heat flow (dQ/dt) must cross through an interface characterised by a heat exchange surface area A:

$$dQ/dt = U.A.\Delta T \qquad (1)$$

U: specific heat transfer coefficient ($W.m^{-2}.K^{-1}$); A: heat exchange surface area (m^2).

In practice, Fig. 3 shows how the sensor temperature will nearly join the sample temperature as long as the sample temperature is kept constant. The settling time required for the measurement depends on the final desired accuracy and on the difference between the initial and equilibrium value given by the sensor. Since increasing the initial difference in these values by (100/36,8) = 272% just increases the settling time by one time constant, the initial sensor temperature is not critical for temperature measurements excepted for very thermally insulating materials.

The interesting feature of this figure is to show that a physical time constant is easy to determine for t = 1τ, since for 1, the signal has drifted from its initial value to a little farther than the half distance towards the equilibrium value (63,2% of the initial distance) and thus this value could be determined with a nearly maximum accuracy, since both the origin (initial measurement) and the end point (equilibrium measurement) are at nearly equidistant from the value for which the time t corresponding to the time constant τ must be determined **[3].**

Another interesting aspect is that for t = 3τ, the measured signal value is not farther from the sample value than 0.5% of the initial difference in sensor and sample temperature. Fore this reason, one can generally admit the measurement to become good for an equilibrium value assessment for t = 3τ and is excellent for t > 5τ.

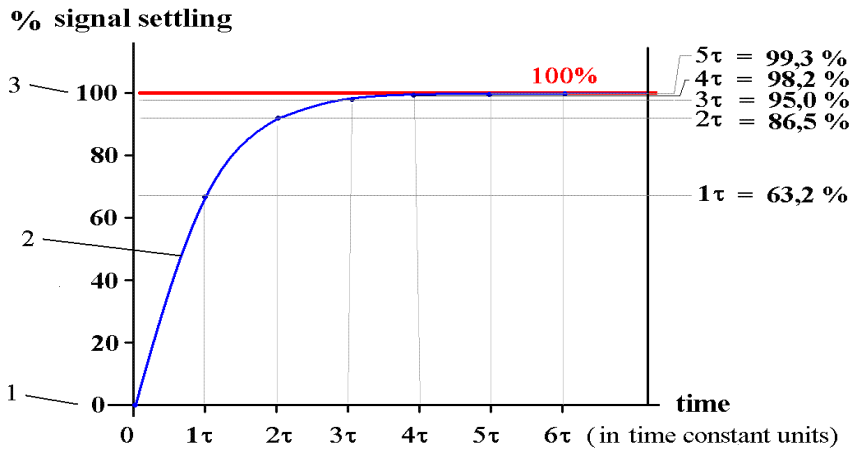

Fig.1: Time dependence of an experimentally measured value while the sensor is settling.

1: initial sensor $T_{ini\text{-}ts}$ value at initial contact time $t_0 = 0$; 2: instantaneous $T_{meas\text{-}ts}$ measured value; 3: actual sample value $T_{sample:}$ expected measured value after sufficient settling time.

At any moment (cf Fig.1), the sample temperature is related to the measured sensor temperature by Eq.(2) where the measured temperature $T_{meas\text{-}ts}$ as given by the sensor must be considered as the initial temperature $T_{ini\text{-}ts}$ of a not yet settled sensor systemso as :

$$T_{sample} = T_{meas\text{-}ts} + [(T_{sample} - T_{ini\text{-}ts})].\exp(-t/\tau)] \qquad (2)$$

Tini-ts : initial sensor temperature before thermal equilibrium is reached (K), Tmeas-s: instantaneous measured temperature (K), T_{sample}: sample temperature (K), t: time (s), τ: time constant (s), $\tau = m_{ts}.Cp_{ts}/U.A$, m_{ts}: temperature sensor mass (g), Cp_{ts} : temperature sensor heat capacity ($J.K^{-1}.g^{-1}$).

In Eq.(2), describes the relation to time the measured temperature $T_{meas\text{-}ts}$ would follow if the sample temperature would remain constant. A thermal signal may be considered as being a succession of instantaneous measurements the *local* evolution of which is described by a succession of local slopes as given by the first derivative of Eq.(1) in which locally both T_{sample} and $T_{meas\text{-}ts}$ are constant. The term (T_{sample} - $T_{ini\text{-}ts}$ describes the error $\Delta T_{sample\text{-}meas}$ induced by the sensor time constant into the measurement of the actual sample temperature T_{sample} , so as one can write Eq.(1) as below (Eq.(2):

$$T_{sample} = T_{meas\text{-}ts} + [(\Delta T_{sample\text{-}meas})] . \exp(-t/\tau)] \quad \textbf{(3)}$$

Therefore, derivation of this function versus time Eq. (2) *in the referential of the measuring sensor* (in which the sensor temperature is considered as the variable magnitude for a *constant sample temperature*) yields the local signal slope given by Eq.(4):

$$(dT_{sample})/dt=[(\Delta T_{sample\text{-}meas})][(-1/\tau).\exp(-t/\tau)] \quad \textbf{(4)}$$

Which is equivalent to:

$$[(-1/\tau)\ (\Delta T_{sample\text{-}meas})].\ \exp(-t/\tau)] = (dT_{sample})/dt \quad \textbf{(5)}$$

Since sample and temperature sensor play symmetrical roles with regard to the settling of the signal, the absolute value of the slope of the instantaneous measured signal in the temperature referential of the sample temperature is the same as the slope of the sample temperature in the referential of the measured temperature, just the signs of both magnitudes are opposite.

Experimentally, since sharp signal shapes can actually be observed by most of the experimental devices at the time scale required by the experiment, such a supplementary correction is generally not required. Thus, the following correction Eq. (6) which is easy to carry out yields excellent correction of signals where more than usual accurate signal shape is required. Such a correction is possible each time an *active* heat source is connected with a *passive* heated device. The instantaneous slope of the temperature versus time of the passive device indicates whether and how much the source is warmer or cooler than the passive device **[4].**

$$T_{sample} = T_{meas\text{-}ts} + \tau\ (dT_{sample})/dt \quad \textbf{(6)}$$

Moreover, some commercial reaction calorimeters provide the possibility of generating a square signal pulse of well known energy. The determination of the time constant becomes thus much easier by just considering the onset and the signal end of the generated square signal.

3. Experimental results and discussions.

The field concerned by the topics discussed in this contribution is extremely broad. On hand of some typical examples, we will try here to illustrate some aspects discussed above.

3.1. DSC study for storage temperature thermal stability determination.

This study will be taken as an example of an organic solid state fine powdered compound (oxime), the exact nature of which cannot be published for industrial confidentiality reasons. However, the confidentiality limitation is of no importance in this study that only focuses on thermo-analytical aspects. The problem was to determine the critical storage size as defined by Frank-Kammenetski's equation **[5]**. Therefore, one had to determine the thermal stability of the product for usual storage temperatures in the range -10 to + 80°C. Its extremely low heat conductivity ($2{,}7.10^{-4}$ $W.K^{-1}.cm^{-1}$) was a critical factor, since large size samples would have resulted in erroneous heat flow determinations as a consequence of possibly undetected thermal heterogeneity of the sample. Further, large size samples could have become dangerous in thermal monitoring *adiabatic* calorimeters (such as Thermal Monitor by TA INTRUMENTS). Since the adiabatic temperature rise of the product induced by total thermal decomposition was higher than 700K, the total decomposition could be induced by local hot spots starting the first exothermal decomposition close to 120°C and heating the sample up to the next exothermal decomposition as shown on Fig.2. This first thermal decomposition

would have induced the following exothermal decompositions steps with their dangerous correlated temperature and pressure rise.

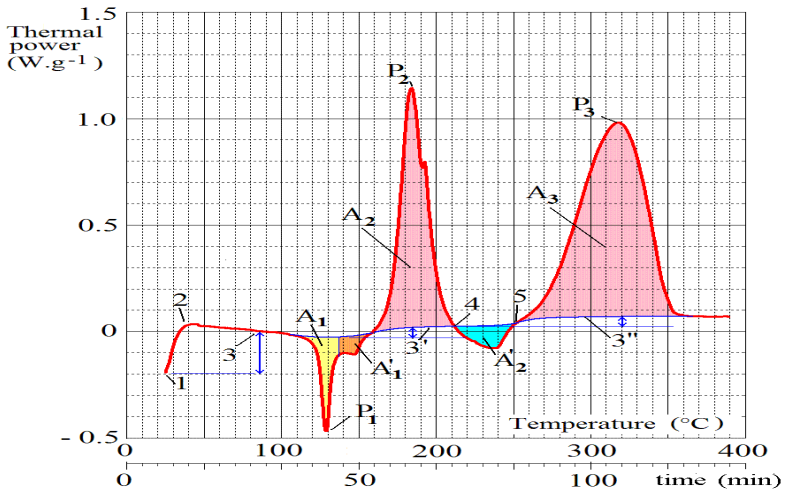

Fig.2: DSC high thermal ramp rate measurement.

Working conditions: DSC calorimeter: NETZSCH DSC 200. **Thermal ramp rate: 3°C/min.**
Sample mass: 5.3 mg . Crucible: sealed gold plated stainless steel. Baseline at: 0.01 mW/mg.
Peak 1 endo: onset: 116.2°C , peak power: - 0.46 W/g , peak energy : - 64.9 J/g.
Peak 2 exo : onset : 147.2°C , peak power : 1.14 W/g , peak energy : 600 J/g .
Peak 3 exo : onset : 239.2°C , peak power : 0.98 W/g , peak energy : 1052 J/g.

On Fig.2 a usual thermal ramp rate (3°C.min^{-1}) results in a noiseless signal with high signal to noise ratios leading to easy to measure thermal powers However, one observes an important baseline drift (mark 3, Fig.2) before the first endothermal peak which a due to melting of the sample. This drift could be assigned to the presence of trace amounts of heptane (less than 1%) in the sample, dissolving partially the main product resulting in changing the heat capacity of the sample while the temperature was rising **[6]**.

The area A'_1 at the end of the endothermal peak is difficult to assign either to the endothermal peak A_1 or to the second exothermal peak P_2. The heating rate being too high, the highly thermally insulating product could not be heated homogeneously: thus, the area A'_1 is attributed to a not yet molten particle hanging somewhere in the upper part of the crucible and dipping into the molten liquid phase while the second exothermal peak P_2 had already started heating up the sample by inside.

At the end of the second peak P_2 (exothermal), an artefact is generated by the fast cooling down of the sample crucible after an important heating phase due to the exothermal transformation corresponding to peak 2. During the exothermal phase, some heat had been transferred from the sample crucible to the reference crucible. Since both reference and sample contained some powdered alumina in order to compensate the thermal inertia of the sample at the beginning of the heating ramp rate, after the melting point, the reference contained still a solid powdered phase. But the sample was liquid, giving it a shorter time constant after melting. The following rapid cooling down of the sample associated with a slower cooling down of the reference, which had to eliminate the heat the sample transferred to it during the exothermal peak gives rise to an endothermal artefact (A'_2). The reference crucible became temporarily hotter than the sample, not because of its own heat, but because of the heat accumulated from the other (sample) crucible. Determining the time constants of the different contributions is nearly impossible here as a consequence of the high thermally insulating properties of the sample, which undergo a drastic change after melting, rendering nearly impossible the choice of a convenient reference. The experiment however allowed determining the order of magnitude of both the endothermal and exothermal peaks, with a total exothermicity corresponding to an adiabatic temperature rise close to 800°C.

The second peak P_2 (first exothermal) could manage an adiabatic rise of temperature close to 300°C which in any case, would be sufficient to initiate the third exothermal peak (P_3). This total exothermicity of the thermal decomposition process would generate an adiabatic temperature rise to close to 800K above the initial temperature, which is a temperature that could easily ignite the product on a storage site.

Since the previous ramp rate (3°C/min, Fig.2) resulted in overrunning the system settling time constants, another DCS experiment has thus been carried out at a six time lower heating ramp rate (0,5°/min, Fig.3) :

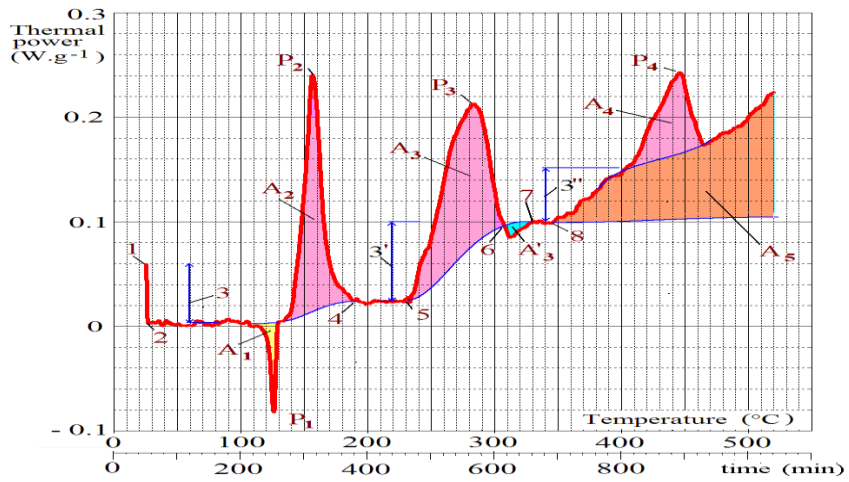

Fig.3: DSC low thermal ramp rate measurement.

Working conditions: DSC calorimeter: NETZSCH DSC 200. **Thermal ramp rate**: **0.5 °C/min**,
Sample mass: 5.9 mg. Crucible: sealed gold plated stainless steel; Baseline at: 0.01 mW/mg,
Peak 1 endo: onset : 113.5°C , peak power : 0.07 W/g , peak energy : - 49.2 J/g
Peak 2 exo: onset : 129.5°C , peak power : 0.25 W/g , peak energy : 482.4 J/g
Peak 3 exo: onset : 232.5°C , peak power : 0.22 W/g , peak energy : 759.2 J/g
Peak 4 exo: onset : 380 °C , peak power : 0.25 W/g , peak energy : 321.7 J/g

On Fig. 3 the low thermal ramp rate (0.5°C.min^{-1}) resulted in a rather noisy signal (with a noise amplitude close to 0.01 W.g^{-1}). However, the loss of information due to this noise was compensated by an excellent resolution of the four peaks appearing in the range 0-500°C of the studied product. The end of peak 1 (Fig. 3) was very sharp, indicating that as soon as the melting process was completed the sample temperature is settled. In other words, all equilibria (as well the transformation going on in the sample as the related heat transfer processes (oven to sample, sample to sensor and sample to environment) were reached in the time range of the experiment without limiting each other : the limiting factor is not the observed phenomena, it is the heating ramp rate. Thus, the results become much clearer than in the previous experiment. However, the measured variations of internal energy are about 20% lower on Fig.8 than on Fig.2: because of the important amplitude of the signals that are far from the instrument standardisation conditions, the heat losses are important. By considering the fact that the NETZSCH 200 calorimeter is a sample bottom temperature measuring instrument, such a behaviour cannot be easily compensated and becomes more important for long duration experiments such as the considered one which lasted for more than 16 hours.

However, on hand of this experiment in a sealed crucible, it became clear that the peak 2 exothermal signal P_2 Fig.3 was induced by the fusion of the product which gives the concerned molecules a energy which is enhanced after the melting point by the heat of fusion as measured by the first peak. This heat of fusion, about (60 $\pm$ 10) J/g would be the potential equivalent of an increased temperature by (30 $\pm$ 5) K if melting would not have taken place for a sample with a heat capacity close to 2 J.K^{-1}g^{-1}. Further, a well-defined baseline separates the end of Peak 2 from the beginning of Peak 3. The onset of peak 3 is sharp, and characterises equilibrium, thermodynamically steered transformation. At the end of peak P_3 however a small endothermal artefact (A'_3) subsists. It probably aroused from the same reasons as the previously observed A'_2 area of Fig.2 that has completely disappeared on Fig.3. The last peak (P_4) of Fig.3 was superimposed over a global thermal decomposition that is difficult to assess because of the uncertainty concerning the baseline position after mark 8, Fig .3. The short (however lasting for nearly 20 min) horizontal line between marks 7 and 8 (Fig.3) is the reason for which the blue baseline was given the shape as shown by Fig.3.

This example illustrates the help of understanding the importance of all heat transfer processes and correlated time constants provides for choosing the best possible working conditions. Although the signal noise becomes important on Fig.3, the signal has a much better time resolution than on Fig.2 (since the temperature ramp rate is six times lower for Fig.8 than for Fig.3, the corresponding signals (heat flows) are reduced by the same ratio). Fig.2 shows a round-shaped pseudo-onset which could give rise to a doubt concerning the possible residual reaction rate at room temperature (0 - 60°C for an industrial storage in European countries) . This doubt would have required a kinetic study with the correlated require determination of activation energies of Peak 3. Since on Fig .2, peak 3 shows smaller slopes than peak 2, one can assume peak 3 to be less temperature sensitive, with a lower activation energy than peak 2. Therefore, residual storage heat build-up by peak 3(Fig.2) would have been more dangerous at room temperature

than for peak 2 (Fig.2). Running the DSC experiment at 0.5 $K.min^{-1}$ (Fig.3) gives clear information upon the fact that the observed peak 2 and 3 (Fig.2) are not kinetically but thermodynamically limited.

***3.2. Total impurity assessment of high purity materials*.**

Alkali metals reacting with organic molecules and more especially with alcohols can result in extremely unstable reaction rates. This is a general behaviour of high purity metal heterogeneous reactions with liquid reagents. Nevertheless, it can become particularly dangerous for alkali metals because of their high reactivity. In order to check the purity of alkali metals the total impurity concentration was lower than a few ppm by weight, and the following experiment was run.

The sodium sample was melted over about 5 hours at a heating rate close to 1.4 $\mu K.s^{-1}$ (nearly 5 mK./h) in a home-made specially designed oven. The sodium containing glass cell was fitted with a K thermocouple plunger. The observed signal was a constant ramp rate before the melting point at a ramp rate close to the oven ramp rate, about $5mK.h^{-1}$ (Fig.4). A round-shaped onset decreases the inner sample temperature ramp rate to approximately 1 $mK.h^{-1}$ for about 5 hours. Then the completely melted sodium changed again its heating ramp rate and follows again the oven temperature (about 5 mK./h). Since between the eutectic melting point and the melting point of pure sodium solid grains, the impurities were totally rejected towards the liquid intergranular phase the midpoint of the observed melting process gave access to the reducing of the cryoscopic lowering of the melting point of the liquid intergranular phase **[7]**.

Sodium sample size 0.100 kg; Sample container: Vacuum sealed Pyrex glass cylinder, external diameter 30 mm, glass thickness 3 mm, length: 300 mm; Heating device: home-made triple active insulating zone oven; Differential temperature sensor : silicon detector (for low thermal noise).

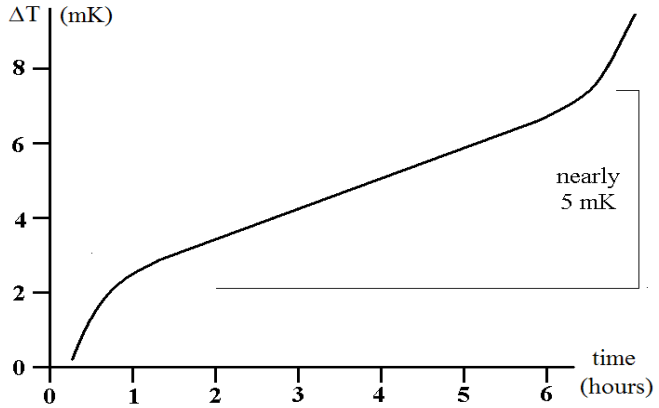

Fig.4: Melting transition of high purity metallic sodium sample (melting point ~ 98°C).

On hand of Raoult's law, one can this way determine the total amount of impurities present in the metallic sodium, regardless to their nature. This illustrates how very particularly thermal analysis interpretation can give important information for special safety requirements related to reaction rate instabilities with too pure reagents.

***3.3. Reaction calorimetry signals*.**

Finally, we will show two examples taken from organic synthesis to show some typical information one can get from reaction calorimetric signals. Both are confidential for industrial reasons, the thermal studies not because the show shapes one could encounter for any similar product **[8, 13].**

***Example 1*.** The first reaction was a substitution reaction of an organic hydrogen atom by liquid bromine following formally Eq. (7):

$$RH + Br_2 \leftrightarrow RBr + HBr \qquad (7)$$

RH , Br_2 and RBr are liquids and soluble in each other HBr is a gas which is soluble in RH but poorly soluble in RBr.

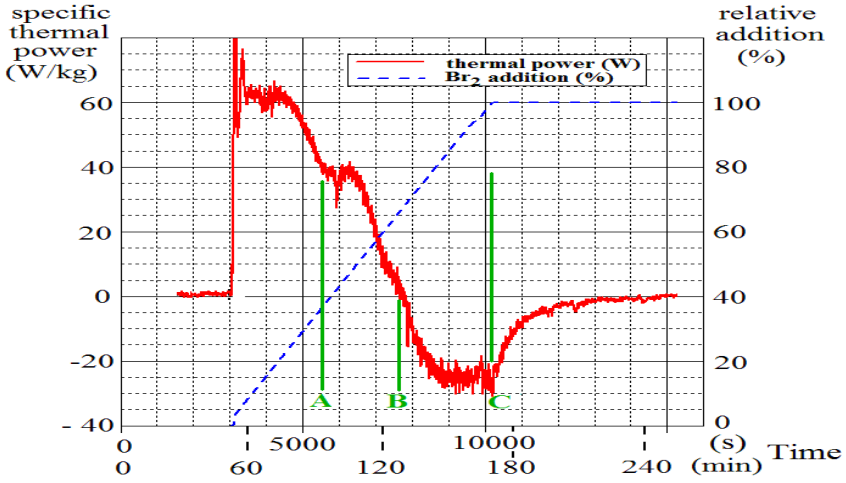

Fig.5: Substitution reaction of an aliphatic hydrogen atom by Bromine.

Reaction calorimeter: Mettler RC-1; Reaction temperature 100°C ± 1°C; Bromine addition: 50% of required stoichiometry per hour; Experiment duration: 2 h.

This experiment ran at constant temperature and constant bromine addition rate, the thermal heat flow underwent extremely important variations along the addition of bromine. The first important aspect was that this reaction was globally nearly a-thermal (neither exo-, nor endothermal): thus if run in a conventional calorimeter mixing in stoichiometric proportions the required amount of organic compound and bromine, one will observe only a very week heat exchange leading possibly to the erroneous conclusion that this reaction is free from any thermal hazard Reaction calorimetry revealed quite the opposite: at the beginning of the reaction, a strong cooling capability was required to keep the temperature constant. Once half the stoichiometric amount of bromine was added, the reaction becomes endothermal and would become extremely slow by cooling down if no complementary heating would keep the temperature constant (Fig.5). Further, this experiment showed also the existence of two reaction mechanisms with different enthalpies. These mechanisms were probably related with the solvation capability of the formed hydrobromic acid HBr with the interacting species the concentration of which varied linearly in time under constant addition rate of bromine : while the initial RH disappeared in the organic phase, the concentration of the final RBr increased so as the total amount of [R]=[RH] + [RBr] remained constant. Thus, RBr will progressively replace the initially bromine and hydrobromic acid solvating medium, which is RH. It appeared clearly on Fig.5 that the initial heat flow that was first stable at about 60W/kg dropped down and remained stable for a similar period at 40 W/kg that is approximately 2/3 of the initial heat flow. This is a clear indication on the existence in the organic medium of well-defined different species formed while the reaction goes on. In its second part, the reaction became endothermal because of the saturation by the hydrobromic acid of the organic liquid. The formation of a gaseous phase lost in its enthalpy for evolving gaseous HBr more energy than the internal energy variation of the condensed phase reaction could provide. The reaction enthalpy became endothermal and complementary heating wass required for completing the reaction.

Example 2. In this example (Fig.6), the reaction ran at constant temperature but at variable HCl addition rate, in order to check for possible reagent accumulation during the addition. Basically, the reaction is Eq. (8):

$$ROH + HCl \leftrightarrow RCl + H_2O \qquad \textbf{(8)}$$

The final product RCl was soluble in the initial alcohol ROH but was not soluble in the final product which was a heterogeneous mixture of a hydrophobic compound (RCl) and a hydrophilic phase wihich contained water (H_2O) and hydrochloric acid (HCl). At its early beginning, the reaction of HCl with the alcohol was instantaneous, which was shown by a constant thermal power between marks A and B. At the mark B, the addition rate was enhanced at twice its initial rate. The heat flow increased but did not rise as expected by raising the addition rate to 100%. This shows that the initial addition rate could not be increased without loosening the advantage of an accumulation free reaction **[9, 10 , 11].** This is confirmed by the inversion of the heat flow slope versus addition at mark B', indicating that the not transformed initial product remaining left at this moment could no longer absorb the added reagent HCl. In order to check at this moment whether a lower addition rate would again result in an accumulation-free reaction, the addition rate was reduced to half the initial value (between marks C and D).

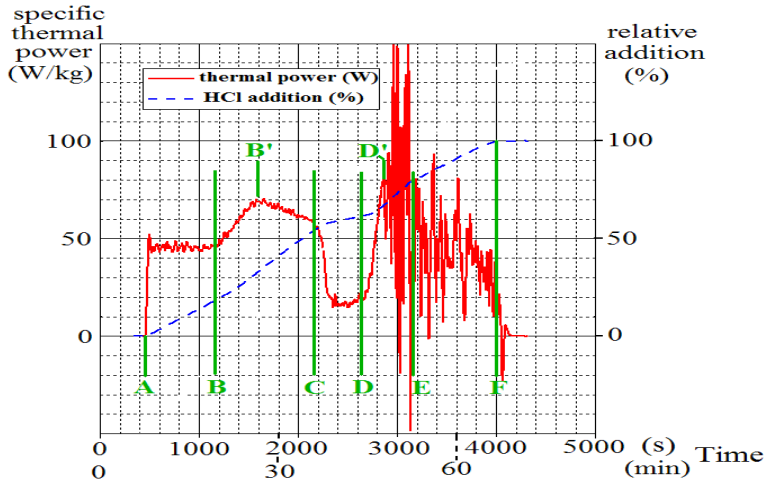

Fig.6: Substitution reaction of an OH group with hydrochloric acid HCl.

Reaction calorimeter : Mettler RC-1; Reaction temperature 10°C ± 1°C; Hydrochloric acid addition : 50% of required stoichiometry per hour; Experiment duration : 1 h.

After a short period over which the reagent consumes the accumulated HCl, the reaction heat flow became again nearly the expected one that is nearly half of the initial heat power. After rising again, the addition rate to twice the initial value a new phenomenon appeared. The heat flow became extremely unstable and a precipitate appeared in the reactor. Thus, the formed product accumulates in the reactor without precipitating until its chemical potential was high enough to compensate the high surface potential of the nano-sized germs required for starting the crystallisation. As soon as the crystal growth starts, crystallisation takes place until the initially oversaturated solution returns back to saturation. Since the reaction mixture was extremely complex other than crystallising molecules would be adsorbed on the surface of the just formed crystals and block thus any complementary growth. The system should start again a nucleation process and strong oscillation of the heat flow of crystallisation goes on (between marks D' and F) until the reaction is completed **[12,14].**

4. Conclusion.

Curvature at onset, baseline offset after peak, baseline drift, signal to noise ratio and settling times are all magnitudes that provide essential information about the phenomena occurring in the calorimeter and in the sample holders (reference). Careful observation of these magnitudes can greatly enhance the quality of signal interpretation. Besides, the most manifested characteristics including amplitude, surface areas and onsets, etc…, are taken into account. Paying attention to the details of the signal shape may also reveal much more information; which generally remain completely hidden at the first glance; such as grain boundary segregation phenomena of impurities in binary systems and surface composition of growing crystals and surface energies of small crystallites. In order to extract as much information as possible from a thermal signal, first be fully aware of all the processes in progress resulting from the transformations induced in the matter by the controlled thermal conditions imposed to the studied sample. This contribution demonstrates certain ways to do so, and some applications of fine observation of details in the thermal measurements for a better interpretation of thermal signals. Additionally, it gives an overview of the reasons why it is necessary to pay attention to the similarity between the samples and the standards, the filling level of the crucibles, their mechanical resistance to internal high pressures and the role of time constants in the accuracy of kinetic measurement. It points out the difference between thermodynamic and kinetic steered system and the potential danger when using apparent kinetic onsets for safety study purposes. It explains how to correctly use this data; not to specify an onset temperature, which is nonsense for kinetically steered transformations, but to evaluate the residual transformation rate at a temperature lower than apparent onset temperature. This is an important concept for the security of applications in the field of chemical storage technology.The final aim is to convince all potential users the power of thermal techniques in order to study the behaviour of the matter, providing that minor aspects are also taken into consideration when analysing the results of thermal measurements.

References.

1. Šesták, J. (1996), Use of phenomenological kinetics and the enthalpy versus temperature diagram (and its derivative-DATA) for a better understanding of transition processes in glasses 1, Thermochimica Acta, 280-281, 175-190. https://doi.org/10.1016/0040-6031(95)02641-X.

2. Bard, Allen J., Faulkner, L.R., Leddy, J., Zoski, C.G. (2001), Electrochemical methods: Fundamentals and applications, John Wiley & Sons, 2nd ed., New York, 105-106.
3. Materazzi, S., Vecchio, S. (2013/04), Thermal analysis and health safety. Journal of Thermal Analysis and Calorimetry, 1125(1), 529-533. https://doi.org/10.1007/s10973-012-2762-z
4. Cheblia, K., Saitera, J.M., Grenet, J., Hamou, A., Saffarini, G. (2001), Strong-fragile glass forming liquid concept applied to GeTe chalcogenide glasses. Physica B: Physic of Condensed Matter, 304, (1-4), 228-236. https://doi.org/10.1016/S0921-4526(01)00501-4.
5. Uyanik, M., Ishihara,K. (2014), Functional Group Transformations via Carbonyl Derivatives Comprehensive Organic Synthesis, 2nd. Edition, 6, 573-597.
6. Hadj Mebarek, A., Walter, S., Diyani, S. (1997), Preparation of high purity alkali metals by near melting point segregation. Journal of Thermal Analysis and Calorimetry, 49, 1283-1288. https://doi.org/10.1007/bf01983685.
7. Walter, S., Aleboyeh, A. (1996), Near melting point flow injection : a drastic enhancement in FAAS detection limits. Fresenius' Journal of Analytical Chemistry, 355, 687-689. https://doi.org/10.1007/s0021663550687.
8. Diyani, S., Walter, S., Hadj Mebarek, A. (1997), Water assisted thermal segregation. A new way for high purity material preparation. Journal of Thermal Analysis and calorimetry, 49, 1289-1296. https://doi.org/10.1007/bf01983686.
9. Lipták, Bela. G. (2003), Instrument Engineers Handbook: Process control and optimization , fourth ed., CRC Press, 100.
10. Lewis, R.W., Nithiarasu, P. Seetharamu., K.N. (2004), Fundamentals of the finite element method for heat and fluid flow, John Wiley and Sons, 151.
11. Rouquerol, J. (1997), Controlled rate evolved gas analysis: 35 years of rewarding services. Thermochimica Acta, 300(1-2), 247- 253. https://doi.org/10.1016/S0040-6031(97)00031-2.
12. Vyazovkin, S., Clawson, J. S., Wight, C. A. (2001), Thermal Dissociation Kinetics of Solid and Liquid Ammonium Nitrate. Chemical Mater, 13, 960-966. https://doi.org/10.1021/cm000708c.
13. Jhu-Ling, J., Hung-Yi, H. (2021), Investigation of thermal risk assessment and hazard rankings for three organic peroxides: DTBP, CHP, and DCPO. Journal of Loss Prevention in the Process Industries, 69, 104335.
14. Ryabchenko, E.V., Mindubaev, E. A., Danilov, A. A. (2022), Rapid Assessment of the Thermal Safety of Low-Frequency Inductive Power Transfer Systems for Implantable Devices. Biomedical Engineering, 56, 185–189. https://doi.org/10.1007/s10527-022-10195-2.